

This item was submitted to [Loughborough's Research Repository](#) by the author.  
Items in Figshare are protected by copyright, with all rights reserved, unless otherwise indicated.

## **Nonlinear free surface flows past a semi-infinite flat plate in water of finite depth**

PLEASE CITE THE PUBLISHED VERSION

LICENCE

CC BY-NC-ND 4.0

REPOSITORY RECORD

Maleewong, Montri, and Roger H.J. Grimshaw. 2019. "Nonlinear Free Surface Flows Past a Semi-infinite Flat Plate in Water of Finite Depth". figshare. <https://hdl.handle.net/2134/2969>.

# Nonlinear free surface flows past a semi-infinite flat plate in water of finite depth

M. MALEEWONG<sup>1</sup> AND R.H.J. GRIMSHAW<sup>2</sup>

<sup>1</sup>Department of Mathematics, Faculty of Science, Kasetsart University, Bangkok, Thailand

<sup>2</sup>Department of Mathematical Sciences, Loughborough University,  
Loughborough, LE11 3TU, UK

(Received ?? and in revised form ??)

We consider the steady free surface two-dimensional flow past a semi-infinite flat plate in water of a constant finite depth. The fluid is assumed to be inviscid, incompressible and the flow is irrotational; surface tension at the free surface is neglected. Our concern is with the periodic waves generated downstream of the plate edge. These can be characterized by a depth-based Froude number,  $F$ , and the depth  $d$  (draft) of the depressed plate. For small  $d$  and subcritical flows, we may use the linearized problem, combined with conservation of momentum, to obtain some analytical results. These linear results are valid when  $F$  is not close to 0 or 1. As  $F$  approaches 1, we use a weakly nonlinear long-wave analysis, and in particular show that the results can be extended to supercritical flows. For larger  $d$  nonlinear effects need to be taken account, and so we solve the fully nonlinear problem numerically using a boundary integral equation method. Here the predicted wavelength from the linear and weakly nonlinear results is used to set the mean depth condition for the nonlinear problem. The results by these three approaches are in good agreement when  $d$  is relatively small. For larger  $d$  our numerical results are compared with known results for the highest wave. We also find some wave-free solutions, which when compared with the weakly nonlinear results are essentially just one-half of a solitary wave solution.

---

## 1. Introduction

Two-dimensional free surface flows past a fixed surface-piercing obstacle is a challenging analytical and numerical problem, relevant to the generation of bow and stern flows in ship hydrodynamics. Our concern here is with the waves generated downstream, and so we assume that the obstacle is semi-infinite. In general, there are strong singularities at the intersection of the free surface with the rigid obstacle, causing difficulties for both analytical and numerical methods. But here, however, we assume that the flow leaves the obstacle tangentially, and then we are able to represent the obstacle as a semi-infinite flat horizontal plate. We will assume that the fluid is inviscid and incompressible with constant density, and that the flow is steady and irrotational.

In water of infinite depth, Schmidt (1981) considered the linearized problem stern flow when the free surface leaves the plate tangentially, under the assumption that  $V^2/gd \gg 1$ , where  $d$  is the draft and  $V$  is the downstream flow speed. An exact solution was found which showed that periodic sine waves are found in the downstream far-field. The corresponding nonlinear problem was considered by Vanden-Broeck (1980) using a boundary integral equation method. For small drafts, the results agreed with the linear theory, but as the draft increases (that is the draft-based Froude number  $V/(gd)^{1/2}$

decreases), the waves steepen and eventually reach the highest possible wave. On the other hand Andersson & Vanden-Broeck (1996) considered an analogous problem for bow flows with surface tension included but gravity neglected. They found that flows with waves do not leave the plate tangentially.

In water of finite depth, the linearized problem was recently considered by McCue & Stump (2000), who assumed that  $d/D \ll 1$  where  $D$  is the downstream mean fluid depth, but the Froude number  $V/(gD)^{1/2}$  is finite. An exact solution was found using the Wiener-Hopf technique, which yielded the expected linear sine waves far downstream for subcritical flows. They also found wave-free supercritical solutions, but these had a singularity at the plate edge. They conjectured that wave-free solutions could only be found when the Froude number and draft satisfy a certain special relationship, predicted by Vanden-Broeck & Keller (1987) using a conservation of momentum argument (see our discussion below). Detaching wave-free stern flows from an inclined plate have been calculated numerically by Hocking (1993). Recently, the generation of capillary waves past by flow past a flat plate have been considered by Tooley & Vanden-Broeck (2004). They found a three-parameter family of solution which are in general characterized by a discontinuity in slope at the separation point.

In this paper, we consider free surface flows past a semi-infinite horizontal plate depressed into water of finite depth. Gravity is included but surface tension is neglected. This is the nonlinear counterpart of the linear problem considered by McCue & Stump (2000). In Section 2 the problem formulation is presented. Then in Section 3 we revisit some aspects of the linearized theory. When the Froude number approaches unity, the periodic waves generated have very long wavelengths, and so, again in Section 3, we present a weakly nonlinear long-wave analysis. Some details of our numerical method are presented in Section 4, but see Maleewong *et al.* (2005) for a full description. In Section 5 we present our numerical results, which for small drafts are compared with the linearized theory, or with the weakly nonlinear long-wave theory when the Froude number approaches unity. As the draft increases, so does the wave steepness, and we can numerically calculate periodic waves, with narrow crests and broad troughs, close to the results for the highest waves obtained by Cokelet (1977). We conclude with Section 6.

## 2. Formulation

We consider two-dimensional flow past a semi-infinite flat plate in water of finite depth. This stern flow is assumed to separate tangentially from the edge of the plate. The fluid is inviscid and incompressible and the flow is steady and irrotational. Far upstream the flow is uniform with constant velocity  $U$  and constant depth  $H$  (see figure 1). The  $x - y$  coordinate is placed on the bottom where the  $y$  axis is at the point of separation. The plate is depressed from the undisturbed level a distance  $Hd$  (draft, see below for a precise definition) to perturb the free surface and so generate waves downstream.

The flow field is thus represented by a streamfunction  $\psi(x, y)$  which satisfies Laplace's equation in the fluid domain, the velocity field is  $u = \psi_y, v = -\psi_x$ , and the boundary conditions are

$$\psi = -Q, \text{ on } y = 0, -\infty < x < \infty, \quad (2.1)$$

$$\psi = 0, \text{ on } y = H, -\infty < x < 0, \text{ and } y = h, 0 < x < \infty, \quad (2.2)$$

$$\frac{u^2 + v^2}{2} + gh = B, \text{ on } y = h, 0 < x < \infty. \quad (2.3)$$

Here  $Q = UH$  is the (constant) mass flux,  $B$  is the unknown Bernoulli constant,  $y =$

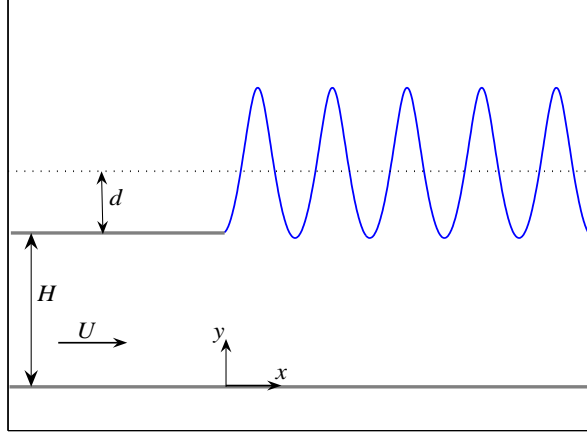


FIGURE 1. Sketch of physical plane

$h(x), x > 0$  is the unknown free surface, and  $u = \psi_y \rightarrow U$  as  $x \rightarrow -\infty$ . Next we impose the condition of tangential separation, namely that  $h_x \rightarrow 0$  as  $x \rightarrow 0+$ . Far downstream we require that the flow is bounded. Because we expect a periodic wave to form far downstream, we introduce the nondimensional draft  $d$  (which can be positive or negative) by requiring that

$$h = H(1 + d) + \hat{h}, \quad \text{where } \langle \hat{h} \rangle = 0, \quad \text{as } x \rightarrow \infty. \quad (2.4)$$

Here  $\langle \dots \rangle$  denotes an average over the periodic wave. But we note that the wavelength for taking this average is still unknown. This issue will be addressed below in Section 4. Next, it is convenient to choose the Bernoulli constant

$$B = \frac{V^2}{2} + g(H + d). \quad (2.5)$$

Here  $V = JU/(1 + d)$  is a measure of the downstream velocity, where we have used conservation of mass to ensure that  $V/U$  scales with  $1/(1 + d)$ . We expect the unknown constant  $J$  to scale with 1 as  $d$  varies, at least for  $d \ll 1$ .

Next we nondimensionalize with  $U, H$  so that (2.1, 2.2, 2.3) become

$$\psi = -1, \quad \text{on } y = 0, \quad -\infty < x < \infty, \quad (2.6)$$

$$\psi = 0, \quad \text{on } y = 1, \quad -\infty < x < 0, \quad \text{and } y = h, \quad 0 < x < \infty, \quad (2.7)$$

$$\frac{F^2(u^2 + v^2)}{2} + h = \frac{J^2 F^2}{2(1 + d)^2} + 1 + d, \quad \text{on } y = h, \quad 0 < x < \infty. \quad (2.8)$$

The two input parameters are now  $F = U/\sqrt{gH}$  and  $d$ . When  $d = 0, J = 1$ , and the solution is the uniform flow  $u = 1, v = 0, h = 1$ . Otherwise  $d \neq 0$  means that the plate at  $y = 0, -\infty < x < 0$  has been depressed a distance  $d$  relative to the flow as  $x \rightarrow \infty$ .

If the downstream state is wave-free, then we must set  $J = 1$  to conserve mass, and there is then an additional boundary condition as  $x \rightarrow \infty$ , namely  $h \rightarrow 1 + d, u \rightarrow 1/(1 + d), v \rightarrow 0$ . This extra constraint means that a solution can only exist for a special relationship between  $F$  and  $d$ , so only one of these can be specified *a priori*. In section 3.1 below we use conservation of momentum to determine this relationship, following

Vanden-Broeck & Keller (1987). Otherwise, when the downstream state contains waves, both  $F$  and  $d$  must be specified *a priori*, and  $J$  is determined as part of the solution.

### 3. Analysis

#### 3.1. Conservation of momentum

In dimensional variables the expression for conservation of momentum is

$$\int_0^{(H,h)} \left( \frac{p}{\rho} + u^2 \right) dy = \text{constant}, \quad \text{for } (-\infty < x < 0, 0 < x < \infty), \quad (3.1)$$

$$\text{where } \frac{p}{\rho} = B - \frac{u^2 + v^2}{2} - gy. \quad (3.2)$$

Here  $p$  is pressure and  $\rho$  is the (constant) density. Substituting for the pressure, using our nondimensional variables and evaluating the constant upstream we get

$$(1, h) \left( \frac{J^2 F^2}{2(1+d)^2} + 1 + d \right) - \frac{(1, h^2)}{2} + \frac{F^2}{2} \int_0^{(1,h)} (u^2 - v^2) dy \quad (3.3)$$

$$= \frac{J^2 F^2}{2(1+d)^2} + \frac{F^2}{2} + d + \frac{1}{2}. \quad (3.4)$$

But then, if there is uniform flow downstream, so that  $(u, v) \rightarrow (1/1+d, 0)$  and  $h \rightarrow 1+d$ , we can also evaluate this expression as  $x \rightarrow \infty$  to get

$$\begin{aligned} (1+d) \left( \frac{F^2}{2(1+d)^2} + 1 + d \right) - \frac{(1+d)^2}{2} + \frac{F^2}{2(1+d)} \\ = \frac{F^2}{2(1+d)^2} + \frac{F^2}{2} + d + \frac{1}{2}. \end{aligned}$$

This is the required relationship between  $F$  and  $d$ . Simplifying it becomes

$$F = 1 + d, \quad (3.5)$$

This is the same result as that found by Vanden-Broeck & Keller (1987), expressed in this present notation. Note that in terms of the downstream Froude number this condition is  $G = 1/(1+d)^{1/2}$ , which is subcritical. That is, the only wave-free flow occurs for *subcritical* downstream conditions.

Next, we consider the general case when periodic waves are generated downstream. That is, as  $x \rightarrow \infty$  there will a uniform periodic wave train. In this situation, we need to define the constants  $J, d$  in a different way. We write

$$u = \frac{K}{1+d} + \hat{u}, \quad h = 1 + d + \hat{h}, \quad (3.6)$$

useful in  $x > 0$  and in particular as  $x \rightarrow \infty$  where  $\hat{u}, \hat{h}$  define the periodic wave. In this case, we now *define*  $d$  by the requirement that  $1+d$  is the mean level, so that  $\hat{h}$  has zero mean, see (2.4). Similarly  $K$  is defined so that  $\hat{u}$  also has zero mean, noting that the mean flow must be a constant, independent of  $y$ . This in effect then determines the constant  $J$ . But only one of the pair  $J, d$  can be imposed *a priori*. We will choose  $d$  to be an input parameter, along with  $F$ , and then  $J$  is determined as part of the solution. In effect, the Bernoulli constant then becomes part of the solution. Note that it will be useful to define a downstream Froude number as  $G = U_m / \sqrt{gH(1+d)} = KF/(1+d)^{3/2}$  where  $U_m = \langle u \rangle$  is the mean velocity in dimensional coordinates.

It is now useful to consider the conservation of mass,

$$\int_0^h u \, dy - 1 = K - 1 + \frac{K\hat{h}}{1+d} + \int_0^h \hat{u} \, dy = 0, \quad (3.7)$$

valid in  $x > 0$ . As before, let  $\langle \cdots \rangle$  denote an average over the periodic wave as  $x \rightarrow \infty$ , so that we get

$$K - 1 = - \langle \int_{1+d}^{1+d+\hat{h}} \hat{u} \, dy \rangle. \quad (3.8)$$

Note that the right-hand side is second-order in the wave-amplitude, but is not zero. To see this, now substitute the expressions (3.6) into the Bernoulli relation (2.8) to get

$$\frac{KF^2}{1+d}\hat{u} + \hat{h} + \frac{F^2}{2}(\hat{u}^2 + v^2) = \frac{F^2}{2(1+d)^2}(J^2 - K^2), \quad (3.9)$$

$$\text{on } y = 1 + d + \hat{h}, 0 < x < \infty. \quad (3.10)$$

We can use this to evaluate  $\hat{u}$  on the free surface, and so eventually get

$$K - 1 = \frac{1+d}{F^2} \langle \hat{h}^2 \rangle + \cdots, \quad (3.11)$$

correct to the second order in the wave-amplitude  $a$  (defined below). Then we use the Bernoulli relation again to show that

$$J = K + \frac{1}{2}(1+d)^2 \langle \hat{u}^2 - v^2 \rangle + \cdots, \quad (3.12)$$

where here  $\hat{u}, v$  are evaluated at the free surface before averaging. Again, this expression is correct to second order in the wave-amplitude. This expression confirms that for a given pair  $(F^2, d)$ ,  $J$  must be determined as part of the solution.

We can now return to the the momentum conservation law (3.4) to determine the wave amplitude downstream. Substitution into the momentum conservation law for  $x > 0$  yields, correct to second order in wave amplitude,

$$-\frac{\hat{h}^2}{2} + \frac{F^2}{2} \int_0^{1+d} (\hat{u}^2 - v^2) \, dy = \frac{F^2}{2(1+d)^2}(d^2 - d(J^2 - 1)) - \frac{d^2}{2}. \quad (3.13)$$

The uniform-flow result (when  $J = 1$ ) follows immediately, as the left-hand side then goes to zero as  $x \pm \infty$ . Otherwise we must evaluate these expressions for the periodic wave solution as  $x \rightarrow \infty$ . For this purpose we now consider the linearized regime in section 3.2.

### 3.2. Linearized theory

The linearized boundary conditions in  $x > 0$  are

$$v = \frac{\hat{h}_x}{1+d}, \quad \frac{F^2}{1+d}\hat{u} + \hat{h} = 0, \quad \text{for } y = 1 + d. \quad (3.14)$$

Here we have used the result that  $J = K = 1$  to the leading order in the wave amplitude. We seek solutions of the form

$$\hat{h} = a \operatorname{Re}[\exp(ik\{x - x_0\})]. \quad (3.15)$$

Here  $a$  is the real-valued amplitude we seek,  $k$  is the wavenumber so that the wavelength  $\lambda = 2\pi/k$ , and  $x_0$  is the phase. We will now show that the amplitude can be determined from momentum conservation, but that the phase can only be found by matching with

the solution in  $x < 0$  and in particular using the constraint that  $h = 1, \hat{h} = -d$  at  $x = 0$ . It now readily follows that the wavenumber  $k$  is given by the linear dispersion relation

$$\frac{F^2}{(1+d)^2} = \frac{\tanh(k(1+d))}{k}. \quad (3.16)$$

Strictly speaking we should also put  $d = 0$  in this expression, as the linearization only holds for  $d \ll 1$ . Also we have

$$\hat{u} = -\frac{ak}{1+d} \frac{\cosh(ky)}{\sinh(k(1+d))} \text{Re}[\exp(ik\{x - x_0\})], \quad (3.17)$$

with a similar expression for  $v$ . We can now evaluate the left-hand side of the momentum conservation law to get, correct to second order in wave amplitude,

$$\frac{a^2}{4} \left[ 1 - \frac{2k(1+d)}{\sinh(2k(1+d))} \right] = \frac{d^2}{2} \left( 1 - \frac{F^2}{(1+d)^2} \right). \quad (3.18)$$

This shows, as expected, that for a fixed  $F$ , the amplitude  $a$  scales with  $d$  when  $0 < d \ll 1$ , and in general, for a fixed  $d$  gives the expression for the variation of  $a$  with  $F$ . The expression is complicated because the wavenumber  $k$  is given in terms of  $F$  by the dispersion relation. But note that the left-hand side is always positive, so we must always have  $F < 1 + d$ , or the downstream Froude number  $G < K/(1+d)^{1/2}$  as expected here for subcritical flow. For simplicity, now let  $d \rightarrow 0$  so that the final formula is

$$\frac{a^2}{4} \left[ 1 - \frac{2k}{\sinh(2k)} \right] = \frac{d^2}{2} \left( 1 - \frac{\tanh(k)}{k} \right), \quad (3.19)$$

$$\text{where } F^2 = \frac{\tanh(k)}{k}. \quad (3.20)$$

This result is plotted in figures 2 and 3 for the case  $d \rightarrow 0$ . We see that the amplitude is predicted to decrease as the Froude number increases. These results agree completely with McCue & Stump (2000), as we can write

$$\frac{a^2}{d^2} = \frac{2F^2(1-F^2)}{F^2 + k^2F^4 - 1},$$

which is precisely the expression found by them, by a much more complicated method.

There are two anomalies with this estimate. First, as  $F \rightarrow 1$ ,  $k \rightarrow 0$  and so a long-wave analysis is needed. This follows below in section 3.3. Second, as  $F \rightarrow 0$ , the prediction is that the wave amplitude  $a/d \rightarrow \sqrt{2}$  remains finite, but that the wavenumber  $k \rightarrow \infty$ ; thus the wave steepness increases, and the linearization fails, except for very small  $d$ . Indeed, for  $F \rightarrow 0$  the present non-dimensional variables are not appropriate, and a rescaling is needed. In essence, the waves become short, do not feel the bottom, and a rescaling is needed in which  $U^2/g$  is the relevant length scale. Thus we rescale the (nondimensional) variables as follows

$$(x, y - 1) = F^2(\hat{x}, \hat{y}), \quad \psi = F^2\hat{\psi}, \quad h - 1 = F^2\hat{h}, \quad d = F^2\hat{d}. \quad (3.21)$$

The boundary conditions now become

$$\hat{\psi}_{\hat{x}} = 0, \text{ on } y = -\frac{1}{F^2}, -\infty < \hat{x} < \infty, \quad (3.22)$$

$$\hat{\psi} = 0, \text{ on } \hat{y} = 0, -\infty < \hat{x} < 0, \text{ and } \hat{y} = \hat{h}, 0 < \hat{x} < \infty, \quad (3.23)$$

$$\frac{u^2 + v^2}{2} + \hat{h} = \frac{J^2}{2(1 + F^2\hat{d})^2} + \hat{d}, \text{ on } \hat{y} = \hat{h}, 0 < \hat{x} < \infty. \quad (3.24)$$

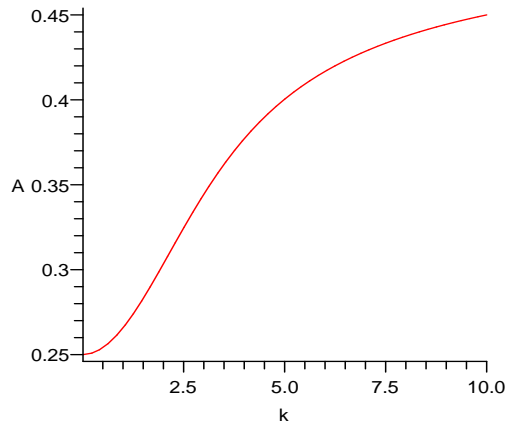


FIGURE 2. Plot of  $A = a^2/4d^2$  against  $k$  for the case  $d \rightarrow 0$ .

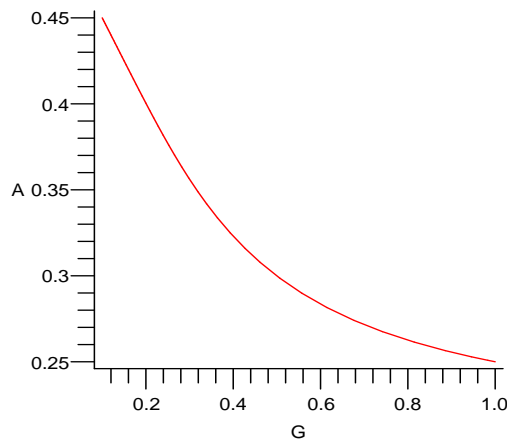


FIGURE 3. Plot of  $A = a^2/4d^2$  against  $E = F^2$  for the case  $d \rightarrow 0$ .

Letting  $F^2 \rightarrow 0$  yields the deep-water formulation, studied by Vanden-Broeck (1980) The significant point that emerges from this work is that solutions will exist only for some finite range  $0 < \hat{d} < d_M = 0.44$ . This means that  $d/F^2$  is bounded as  $F^2 \rightarrow 0$ , and so solutions can only be found for increasing;y small values of  $d$  as  $F \rightarrow 0$ .

A related aspect that emerges in the fully nonlinear problem is that the solutions will be limited by the wave of maximum amplitude  $a_M$ . From the numerical results of Cokelet (1977) for periodic waves (see section 3.5)  $2a_M/\lambda = 0.141055$  in deep water, while in shallow water  $a_M/1 + d = 0.447$ . These can be translated to limiting wave amplitudes as functions of the Froude number, that is we estimate that  $a_M = 0.443F^2$  for deep water ( $F^2 \rightarrow 0$ ) and also that  $a_M = 0.44$  for shallow water ( $F^2 \rightarrow 1$ ). In fact it would seem that a good estimate is  $a_M = 0.44F^2$  for all  $F^2 < 1$ .

## 3.3. Long-wave analysis

To describe weakly nonlinear long waves, we introduce the scaling, for

$$X = \epsilon x, \quad h = 1 + d + \epsilon^2 H(X), \quad F^2 = (1 + d)^3 + \epsilon^2 \Delta, \quad d = \epsilon^2 D. \quad (3.25)$$

Note that we are expanding about the downstream flow in the region  $X > 0$ . The corresponding expansion for  $u, v$  are

$$u = \frac{K}{1 + d} + \epsilon^2 U(X) - \epsilon^4 \frac{y^2}{2} U_{XX} + \dots, \quad (3.26)$$

$$v = -\epsilon^3 y U_X + \dots, \quad (3.27)$$

$$(J, K) = 1 + \epsilon^4 (M, N) + \dots. \quad (3.28)$$

It can be shown that there are no  $O(\epsilon^2)$  term in the expansions for  $(J, K)$ . Substitution into the integral expression for conservation of mass (3.7) yields

$$H + U(1 + d)^2 + \epsilon^2 (UH - \frac{1}{6} U_{XX}) + \dots = -\epsilon^2 M, \quad (3.29)$$

while the Bernoulli condition (2.8) yields

$$H + U(1 + d)^2 + \epsilon^2 (\Delta U + \frac{U^2}{2} - \frac{1}{2} U_{XX}) + \dots = \epsilon^2 \frac{N}{2}. \quad (3.30)$$

Subtraction yields, as expected, the steady-state Korteweg-de Vries (KdV) equation

$$\Delta U + \frac{3}{2} U^2 - \frac{1}{3} U_{XX} = \frac{3N}{2}, \quad (3.31)$$

$$\text{or } -\Delta H + \frac{3}{2} H^2 + \frac{1}{3} H_{XX} = \frac{3N}{2}. \quad (3.32)$$

Note that  $U = -H$  to leading order. The constant  $N$  is determined as before, that is  $N = \langle H^2 \rangle$  (so that  $N > 0$ ) for a periodic solution. But if we impose the condition that  $H \rightarrow 0$  as  $X \rightarrow \infty$ , then  $N = 0$ . Later we will also impose the boundary condition  $H = -D, H_X = 0$  at  $X = 0$ . This ensures a unique solution, and the issue is then how this behaves as  $X \rightarrow \infty$ .

One integration gives

$$\frac{H_X^2}{3} - \Delta H^2 + H^3 = 3NH + C, \quad (3.33)$$

where  $C$  is a constant. First let us consider the periodic wave solution given by

$$H = A + a \text{cn}^2(\gamma(X - X_0)), \quad (3.34)$$

$$\text{where } a = \frac{4}{3} m \gamma^2, \quad 3A = \Delta - \frac{a}{m} (2m - 1), \quad (3.35)$$

$$3N = 3A^2 - 2\Delta A + \frac{a^2}{m} (1 - m), \quad (3.36)$$

$$\text{and } C = -2A^3 + \Delta A^2 - A \frac{a^2}{m} (1 - m). \quad (3.37)$$

Here  $\text{cn}(\gamma X)$  is a Jacobian elliptic function of modulus  $m$  ( $0 < m < 1$ ). This solution contains four parameters,  $A, a (> 0), \gamma, m$  as well as the phase shift  $X_0$ , and the spatial wavelength is

$$\lambda = \frac{2K(m)}{\gamma}, \quad (3.38)$$

where  $K(m)$  is the complete elliptic integral of the first kind. From (3.35) we see that there are two free parameters, say  $a, m$ , for each fixed value of  $\Delta$ . But the definition of  $D$  requires that we impose the condition that  $\langle H \rangle = 0$  and so

$$A = -\langle a \operatorname{cn}^2(\gamma(X - X_0)) \rangle = -\frac{a}{m} \left[ \frac{E(m)}{K(m)} - 1 + m \right], \quad (3.39)$$

$$\text{where now } \frac{a}{m} = \frac{4\gamma^2}{3}, \quad \Delta = \frac{a}{m} \left[ 2 - m - \frac{3E(m)}{K(m)} \right]. \quad (3.40)$$

$$3N = \frac{a^2}{m^2} \left[ m - 1 + \frac{2E(m)}{K(m)}(2 - m) - \frac{3E(m)^2}{K(m)^2} \right], \quad (3.41)$$

$$\text{and } C = -A \frac{a^2}{m^2} \left[ \frac{E(m)}{K(m)} - \frac{E(m)^2}{K(m)^2} \right]. \quad (3.42)$$

This condition reduces the family to a one-parameter family. We note that  $A < 0$ , and that as a consequence we must have  $C > 0$  as well as  $N > 0$ . It can be shown that these conditions hold in the expressions above for all  $0 < m < 1$ . Further it can also be shown that if we write  $\Delta = (a/m)\Phi(m)$ , then  $\Phi(m)$  varies monotonically from  $-1$  to  $1$  as  $m$  increases from  $0$  to  $1$ , where the zero occurs at  $m = 0.96$ .

Finally we impose the boundary condition that  $H_X = 0, H = -D$  at  $X = 0$ . There are two cases to consider. First consider the solution  $A = -D$  and  $\gamma X_0 = K(m)$  so that

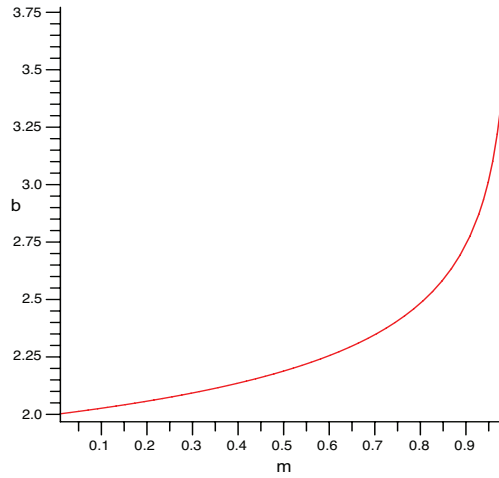
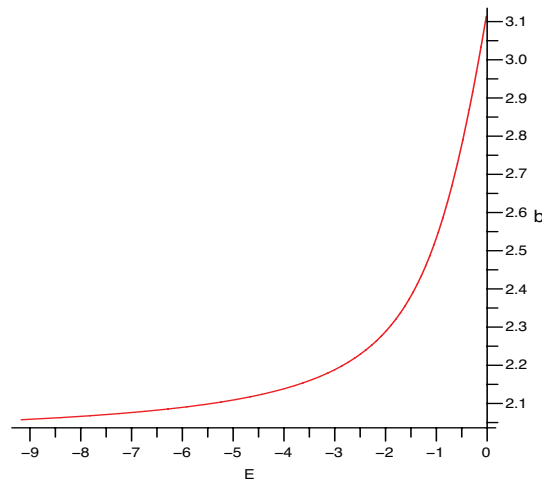
$$D = \frac{a}{m} \left[ \frac{E(m)}{K(m)} - 1 + m \right]. \quad (3.43)$$

Thus, for a given  $D$  (3.43) and  $\Delta$  (3.40), we can determine  $a, m$  and hence all the parameters in the periodic wave. Indeed, from (3.43) we can write  $a/D = F(m)$ , where as  $m$  increases in the range  $0 < m < 1$ ,  $F(m)$  increases from  $2$  to  $\infty$  (see figure 4). Since from (3.40)  $a > 0$  it follows that solutions only exist in this case for  $D > 0$ . Further, we see that the ratio  $\Delta/D = G(m)$  and so determines the modulus  $m$ . As  $m$  increases in the range  $0 < m < 1$ , it can be shown that  $G(m)$  increases monotonically from  $-\infty$  to  $\infty$ , with a zero at  $m = 0.96$ . It follows that there is a unique solution for all  $\Delta, D(> 0)$ , where for a fixed  $D$ ,  $\Delta$  increases from  $-\infty$  to  $\infty$ . In figure 5 we plot  $a/D$  as a function of  $\Delta/D$ . The wavenumber  $\gamma$  is given by  $4\gamma^2/3D = F(m)/m$ , and for a fixed  $D$  decreases from  $\infty$  to  $0$  as  $m$  increases. Further, it then follows that the spatial wavelength (3.38) increases from  $0$  to  $\infty$  as  $m$  increases with  $D$  fixed. As  $m \rightarrow 0$ ,  $a \sim 2D$ ,  $\Delta \sim -2D/m$ , the spatial wavelength is  $\pi/\gamma$  where  $4\gamma^2/3 \sim -\Delta$ , and we recover the linear theory (note that  $a$  is here twice the amplitude used previously in the linearised theory of section 3.2). At  $\Delta = 0$ ,  $m = 0.96$  and  $a = 3.13D$ , and the spatial wavelength is  $6.06/\gamma$  where  $\gamma^2 = 2.45D$ . As  $m \rightarrow 1$ ,  $a/D \rightarrow \infty$ ,  $\Delta \sim a$ , and  $4\gamma^2/3 \sim \Delta$ , which is outside the range of this weakly nonlinear theory.

Next, consider the alternative solution  $A + a = -D$  and  $X_0 = 0$ . In this case (3.43) is replaced by

$$-D = \frac{a}{m} \left[ 1 - \frac{E(m)}{K(m)} \right]. \quad (3.44)$$

The analysis proceeds as above, but now  $-a/D = \hat{F}(m)$  where as  $m$  increases,  $\hat{F}(m)$  decreases from  $2$  to  $1$ . Hence, this case exists only for  $D < 0$ . The ratio  $-\Delta/D = \hat{G}(m)$  where as  $m$  increases,  $\hat{G}(m)$  increases from  $-\infty$  to  $1$  as  $m$  increases, with a zero at  $m = 0.96$ . There is a unique solution for all  $\Delta, D(< 0)$  such that  $\Delta/(-D) \leq 1$ , where for a fixed  $D$ ,  $\Delta$  increases from  $-\infty$  to  $-D$ . The wavenumber  $\gamma$  is given by  $4\gamma^2/(-3D) = \hat{F}(m)/m$ , and for a fixed  $D$  this expression decreases from  $\infty$  to  $1$  as  $m$  increases. Further, it then

FIGURE 4. Plot of  $b = a/D$  against  $m$ FIGURE 5. Plot of  $b = a/D$  against  $E = \Delta/D$ .

follows that the spatial wavelength (3.38) increases from 0 to  $\infty$  as  $m$  increases with  $D$  fixed. But here it is important to note that there is a limiting solution as  $m \rightarrow 1$ , which is a solitary wave, of amplitude  $\Delta = -D$ . This limiting solution is a wave-free solution, and is discussed in more detail in the next paragraph.

To seek wave-free solutions directly we must impose the extra boundary condition that  $H \rightarrow 0$  as  $X \rightarrow \infty$ , so that then  $C = N = 0$  and a solution exists only if  $\Delta > 0$ . Then if we also impose the boundary condition at  $X = 0$ , we must have  $\Delta = -D$ , which is just the condition obtained previously for a wave-free solution in the present long-wave limit, that is  $F^2 = 1 + 2\epsilon^2 D + \dots$ . Note that such wave-free solutions exist only if  $D < 0$ . In the unscaled variables  $F^2 = (1 + d)^2$  and  $G^2 = 1/1 + d$ . Since  $d < 0$  the downstream flow is supercritical as expected,  $G > 1$ , but the upstream flow is subcritical,  $F < 1$ . With

$N = C = 0$  (3.33) has the solitary wave solution

$$H = \Delta \operatorname{sech}^2(\gamma(X - X_0)),$$

where  $4\gamma^2 = 3\Delta$ . This can satisfy the boundary condition at the plate edge that  $H_X = 0$ ,  $H = -D$  if  $X_0 = 0$  and  $\Delta = -D$  as expected. As above, we see that this is a limiting solution of a family of downstream periodic waves, obtained as  $\Delta \rightarrow -D$  from below.

#### 3.4. Local analysis at plate edge

Returning to the full problem, we now examine closely the conditions which hold at the edge of the plate, namely near  $y = 1, x = 0$ . Assuming continuity of the elevation and velocity fields, we find from the boundary conditions (2.6, 2.7, 2.8) that

$$h = 1, \quad v = 0 = uh_x, \quad \frac{F^2}{2}u^2 = \frac{J^2 F^2}{2(1+d)^2} + d, \quad (3.45)$$

$$\text{and } F^2(uu_x + uu_y h_x) + h_x = 0. \quad \text{at } y = 1, x = 0. \quad (3.46)$$

where the last condition comes from the derivative of the Bernoulli condition. It follows that here  $u \neq 0$  at the edge of the plate, which is thus not a stagnation point. Then we must also have that  $h_x = u_x = 0$  at  $y = 1, x = 0$ .

Let us take local polar coordinates  $(r, \theta)$  at the plate edge. Then if  $U_0$  is the velocity at the plate edge we expand the stream function, which must satisfy Laplace's equation, as

$$\psi = U_0 r \sin \theta + Cr^{3/2} \cos \frac{3\theta}{2} + Dr^2 \sin 2\theta + Er^{5/2} \cos \frac{5\theta}{2} \quad (3.47)$$

$$+ E_1 r^{5/2} \left\{ \ln r \cos \frac{5\theta}{2} - (\pi + \theta) \sin \frac{5\theta}{2} \right\} \dots \quad (3.48)$$

Then the kinematic condition on the plate is satisfied since  $\psi = 0$  on  $\theta = -\pi$ , while the free surface, where also  $\psi = 0$ , is given by

$$\sin \theta \approx \alpha r^{1/2} + \beta r^{3/2} + \gamma r^{3/2} \ln r, \quad (3.49)$$

$$\text{where } U_0 \alpha + C = 0, \quad U_0 \beta + E + 2D\alpha = \frac{9}{8}C\alpha^2, \quad U_0 \gamma + E_1 = 0. \quad (3.50)$$

Next, the velocity fields are given by

$$\psi_r = U_0 \sin \theta + \frac{3C}{2} r^{1/2} \cos \frac{3\theta}{2} + 2Dr \sin 2\theta + \dots$$

$$\frac{\psi_\theta}{r} = U_0 \cos \theta - \frac{3C}{2} r^{1/2} \sin \frac{3\theta}{2} + 2Dr \cos 2\theta + \dots$$

The Bernoulli condition (2.8) then gives locally, on the free surface,

$$\frac{F^2}{2} \left\{ -3U_0 C r^{1/2} \sin \frac{\theta}{2} + 4U_0 D r \cos \theta + \frac{9}{4} C^2 r + \dots \right\} + r \sin \theta = 0.$$

Substituting the free surface approximation (3.49) into this expression, we get

$$\frac{F^2}{2} \left\{ -3U_0 C \alpha \frac{r}{2} + 4U_0 D r + \frac{9}{4} C^2 r - 5\pi U_0 E_1 r^{3/2} + \dots \right\} + \alpha r^{3/2} + \dots = 0. \quad (3.51)$$

$$\text{so that } U_0 D = -15C^2/16, \quad \alpha = 5F^2 \pi U_0 E_1 / 2. \quad (3.52)$$

Thus, given the leading order coefficient  $\alpha$  in (3.49) we see from (3.50, 3.52) that

$\gamma, C, D, E_1$  are now known, but consideration of higher-order terms is needed to find  $\beta, E$ . Using (3.50) we get

$$\frac{\gamma}{\alpha} = -\frac{2}{5\pi F^2 U_0^2}. \quad (3.53)$$

which agrees with the expression obtained by McCue & Stump (2000) (see their equation (27)), since the free surface in  $x > 0$  is given approximately by

$$h \approx \alpha x^{3/2} + \beta x^{5/2} + \gamma x^{5/2} \ln x.$$

However, this analysis gives no information on even the sign of  $\alpha$  as it is not linked to the upstream and downstream conditions. But it does indicate that the long wave analysis is not strictly valid at  $x = 0$ , as there is a weak singularity at the plate edge.

### 3.5. Comparison with the highest wave

As the draft  $d$  increases in magnitude, so does the amplitude of the periodic waves generated downstream. In the section 5 we will compare our results for the largest waves that we can generate, with the numerical results obtained by Cokelet (1977) for the highest periodic waves. In this subsection, we will describe how we recast Cokelet's results into our present formulation. Cokelet (1977) defined the wave speed  $c$  by requiring that the fluid velocity have zero mean. He also normalized distance with  $1/k_d$ , where the dimensional wavelength is  $\lambda_d = 2\pi/k_d$ , and normalized the speed with  $(g/k_d)^{1/2}$ , where we denote  $k_d$  to be the dimensional wavenumber ( $k$  in Cokelet (1977)). This means in effect that  $c$  is such that  $c(g/k_d)^{1/2} = KU/(1+d)$ , where we recall our decomposition (3.6) into a mean and oscillatory wave, to be used as  $x \rightarrow \infty$ . Also, in Cokelet (1977), the mean (nondimensional) depth  $D = \tilde{d} + \bar{\eta}$ , where we denote his depth by  $\tilde{d}$  to distinguish it from our notation  $d$  (draft), and  $\bar{\eta}$  is the mean free surface elevation. Thus the present Froude number is related to  $c$  by

$$F^2 = U^2/gH = \frac{c^2(1+d)^2}{kK^2}$$

Here we are using a nondimensional  $k = k_d H$ . To use this expression we need to compute  $k = 2\pi/\lambda$  where  $\lambda$  is the wavelength of the highest wave we compute, and then find  $c^2$  from the Appendix of Cokelet (1977). Also, taking account of the different dimensionalizations  $D = k(1+d)$ . Note that the downstream Froude number  $G$  is given by

$$G^2 = \frac{K^2 F^2}{(1+d)^3} = \frac{c^2}{D}$$

. Note that since  $K \approx 1 + O(d^2)$ , this shows that we expect  $F^2 \approx G^2(1+3d)$  for  $d \ll 1$  and in particular we expect that  $F^2 > (<)G^2$  according as  $d > (<)0$ .

From our numerical results (see section 5), we know  $F^2$ ,  $d$  and the amplitude  $a$  (one half of the crest-to-trough distance) of the highest wave found. We also can compute the wavenumber  $k$  from the wavelength  $\lambda = 2\pi/k$  of the highest wave found. The nonlinear factor  $K$  can be found for the highest wave by computing the average speed at any level, say the bottom  $y = 0$ . Or we use the small-amplitude expression (3.11)

$$K = 1 + \frac{(1+d)a^2}{2F^2}$$

which should be reasonable except when  $F^2$  is very small. Thus we can plot a graph of  $2a/\lambda$  versus either  $F^2$ , or better  $G^2$ . The corresponding plot from Cokelet (1977) is found by choosing  $\tilde{d}$  to get  $D = \tilde{d} + \bar{\eta}$ . This then gives his value of the highest wave amplitude  $2a/\lambda$  corresponding to a value of  $G^2 = c^2/D$ .

## 4. Numerical method

### 4.1. Formulation

For the fully nonlinear problem, we use a numerical boundary integral method, similar to that used by Maleewong *et al.* (2005). Here we just present essential details. Since the fluid is incompressible and the flow is irrotational, we can introduce a potential function  $\phi(x, y)$  and a stream function  $\psi(x, y)$  so that the complex potential function is  $f = \phi + i\psi$ , while the complex velocity by  $w = u - iv$ . We recall that the boundary conditions are defined by (2.6, 2.7, 2.8). The numerical method is now formulated in the  $(\phi, \psi)$ -plane, so that  $w = w(f)$ . Without loss of generality, we choose  $\phi = 0$  at the edge of the plate (the separation point). Note that the kinematic condition on the bottom can be written as

$$v(\phi, \psi) = 0 \quad \text{on} \quad \psi = -1. \quad (4.1)$$

We map the complex  $f$ -plane to the complex  $(\alpha, \beta)$  plane by the transformation

$$\zeta = \alpha + i\beta = e^{\pi f}, \quad (4.2)$$

which maps the flow domain in the  $f$ -plane to the lower half of the  $\zeta$ -plane. We define the complex velocity in the  $\zeta$ -plane by

$$w = u - iv = e^{\tau - i\theta}. \quad (4.3)$$

In particular, we have the relations  $\alpha = e^{\pi\phi} \cos(\pi\psi)$  and  $\beta = e^{\pi\phi} \sin(\pi\psi)$ . In the  $\zeta$ -plane, we choose a contour consisting of the real axis and a half-circle of arbitrarily large radius in the lower half plane. Applying the Cauchy integral formula to the function  $\tau - i\theta$  in the complex  $\zeta$ - plane, we get

$$\tau - i\theta = -\frac{1}{2\pi i} \oint \frac{\tau(\zeta') - i\theta(\zeta')}{\zeta' - \zeta} d\zeta' \quad (4.4)$$

The line integral on the path of half-circle vanishes as we let the radius go to infinity. Letting  $\zeta$  approaches the boundary  $\beta = 0$ , we obtain

$$\tau - i\theta = -\frac{1}{\pi i} \int_{-\infty}^{\infty} \frac{\tau(\alpha') - i\theta(\alpha')}{\alpha' - \alpha} d\alpha' \quad (4.5)$$

The real part yields

$$\tau(\alpha) = \frac{1}{\pi} \int_{-\infty}^{\infty} \frac{\theta(\alpha')}{\alpha' - \alpha} d\alpha' \quad (4.6)$$

The kinematic condition on the bottom implies that

$$\theta(\alpha) = 0 \quad \text{for} \quad \alpha < 0 \quad (4.7)$$

Substituting (4.7) into (4.6), we have

$$\tau(\alpha) = \frac{1}{\pi} \int_1^{\infty} \frac{\theta(\alpha')}{\alpha' - \alpha} d\alpha' \quad (4.8)$$

We obtain another relation between  $\tau$  and  $\theta$  on the free surface by using 4.3) to get  $u^2 + v^2 = e^{2\tau}$ . Thus the Bernoulli relation (2.8) becomes

$$\frac{F^2 e^{2\tau}}{2} + y = \frac{J^2 F^2}{2(1+d)^2} + 1 + d. \quad (4.9)$$

Finally, the free surface profile is determined by integrating numerically the identity

$$\frac{dx}{d\phi} + i \frac{dy}{d\phi} = w^{-1} = \frac{\cos(\theta) + i \sin(\theta)}{e^\tau} \quad , , \quad (4.10)$$

$$\text{that is, } \frac{dy}{d\phi} = \frac{\sin(\theta)}{e^\tau} \quad \text{or} \quad \frac{dy}{d\alpha} = \frac{e^{-\tau} \sin(\theta)}{\pi\alpha}. \quad (4.11)$$

Integrating (4.11) yields,

$$y(\alpha) - y(0) = \frac{1}{\pi} \int_1^\alpha \frac{e^{-\tau} \sin(\theta)}{\alpha} d\alpha \quad , \quad 1 < \alpha < \infty. \quad (4.12)$$

Equations (4.8), (4.9) and (4.12) define a nonlinear integral equation for the unknown function  $\theta(\alpha)$  on the free surface.

#### 4.2. Numerical Procedure

We solve the system of integral equations (4.8), (4.9) and (4.12) numerically by placing equally spaced points  $\phi_i$  on  $\psi = 0$ . The transformation from the  $f$ - plane to the  $\zeta$ - plane gives

$$\alpha = e^{\pi\phi} \quad (4.13)$$

We write  $\tau'(\phi) = \tau(e^{\pi\phi})$ ,  $\theta'(\phi) = \theta(e^{\pi\phi})$  and  $y'(\phi) = y(e^{\pi\phi})$  for brevity. Equation (4.8) then becomes,

$$\tau'(\phi) = \int_0^\infty \frac{\theta'(\phi_0) e^{\pi\phi_0}}{e^{\pi\phi_0} - e^{\pi\phi}} d\phi_0 \quad (4.14)$$

Similarly we rewrite (4.9) and (4.12) as

$$F^2 e^{2\tau'(\phi)} + 2y'(\phi) = \frac{J^2 F^2}{(1+d)^2} + 2 + 2d \quad , \quad (4.15)$$

$$y'(\phi) = y'(0) + \int_0^\phi e^{-\tau'(\phi_0)} \sin \theta'(\phi_0) d\phi_0. \quad (4.16)$$

Next we introduce the equally spaced mesh points

$$\phi_i = (i-1)E \quad , \quad i = 1, 2, \dots, M$$

where  $E$  is the discretization interval. We evaluate the values  $\tau_{i+\frac{1}{2}}$  of  $\tau'(\phi)$  in equation (4.14) at the midpoints

$$\phi_{i+\frac{1}{2}} = \frac{\phi_i + \phi_{i+1}}{2} \quad , \quad i = 1, 2, \dots, M-1$$

by using trapezoidal rule with summation over the points  $\phi_i$ . The symmetry of the quadrature and the distribution of mesh points enable us to evaluate the integral which is of Cauchy principal value integral as if it were an ordinary integral. Next we evaluate  $y_i = y'(\phi_i)$  by applying the trapezoidal rule to (4.16) with,

$$y_1 = 1 \quad ,$$

$$\text{where } y_i = y_{i-1} + e^{-\tau_{i-\frac{1}{2}}} \sin(\theta_{i-\frac{1}{2}}) E \quad , \quad i = 2, \dots, M.$$

We use these values to evaluate  $y'(\phi)$  at the midpoints by using a four-point interpolation formula. We now satisfy the free surface condition (4.15) by substituting these values of  $\tau'(\phi)$  and  $y'(\phi)$  at the midpoints. This yields  $M - 1$  nonlinear algebraic equations for the  $M + 1$  unknowns  $\theta_i, i = 1, \dots, M$ , and  $J$ . We require two constraint conditions. One condition is obtained by assuming that the flow separates from the plate tangentially,

$$\theta_1 = 0.$$

The last condition is obtained by imposing the mean depth condition, that is (see (2.4))

$$1 + d = \frac{1}{\lambda} \int_Y^{Y+\lambda} y(\phi) d\phi, \quad Y \rightarrow \infty,$$

The value of  $\lambda$  to be used in this last condition now needs to be specified. Nonlinear periodic water waves are characterized by four parameters, the wavelength, the mean depth, the speed and the wave amplitude. Of these three may be specified *a priori*, and the fourth is then determined (see Cokelet (1977) for instance). Here we will specify the speed through the Froude number  $F$ , the mean depth  $1 + d$  and the wavelength  $\lambda$ , leaving the wave amplitude to be determined. However, the three specified parameters cannot take completely arbitrary values, as they vary only rather limited ranges. This is most easily seen from the small-amplitude limit, when the linear dispersion relation (3.16) (for  $d \neq 0$ ) or (3.20) (when  $d \rightarrow 0$ ) must hold, providing a direct link between the wavelength  $\lambda = 2\pi/k$  and the Froude number. Hence, taking this into account, we used three methods for specifying the input wavelength.

*Method 1:* The linear dispersion relation with ( $d = 0$ ) (3.20) is used:

$$F^2 = \frac{\tanh k}{k}, \quad k = \frac{2\pi}{\lambda}.$$

*Method 2:* The linear dispersion relation with ( $d \neq 0$ ) (3.16) is used:

$$\frac{F^2}{(1+d)^2} = \frac{\tanh k(1+d)}{k}, \quad k = \frac{2\pi}{\lambda}.$$

*Method 3:* We use the weakly nonlinear long-wave analysis of section 3.3, which gives a good approximation when  $F^2 \approx 1$  and  $|d| \ll 1$ .

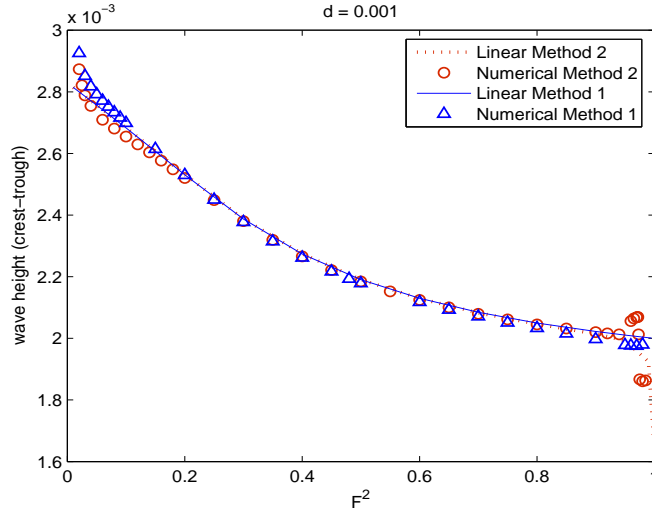
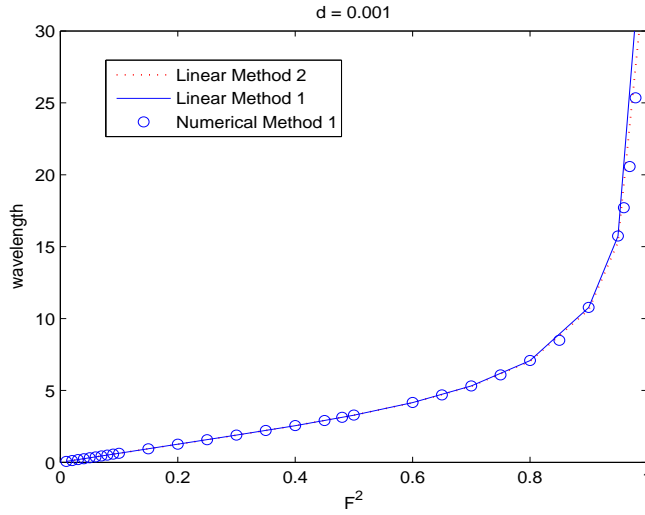
The system of  $M + 1$  nonlinear algebraic equations with  $M + 1$  unknowns is then solved numerically by Newton's Method. The results are described in the next section.

## 5. Numerical Results

### 5.1. Results for small draft

The relationship between the wave height (distant from crest to trough) and  $F^2$  when  $d = 0.001$  is shown in figure 6. For  $d \ll 1$ , the numerical results agree very well with the theoretical results, (3.19) for method 1, or (3.18) for method 2, from the linearized theory of section 3.2, provided that  $F^2$  is not close to 0 or 1. Note that the linearized theory using method 2 has a (spurious) dip in amplitude as  $F \rightarrow 1$ . This in turn affects the amplitude of the numerical solutions obtained by method 2. A plot of the wavelength versus  $F^2$  for  $d = 0.001$  is shown in figure 7. As  $F$  increases, the wavelength of the periodic wave also increases.

To obtain more accuracy of the numerical solutions when  $F^2 \approx 1$ , we used method 3 where the wavelength is found from the long wave analysis. The results are shown in figure 8 where we see that the long wave analysis and the numerical results have the same

FIGURE 6. Relationship between wave height (crest-trough) and  $F^2$  when  $d = 0.001$ .FIGURE 7. Relationship between wavelength and  $F^2$  when  $d = 0.001$ .

trend, and they have good agreement when  $F^2 \approx 1$ , as expected. The analysis in section 3.2 suggests that the linearization fails when  $F \rightarrow 0$ ,  $k \rightarrow \infty$  and so  $\lambda \rightarrow 0$ . A rescaling is needed and it was found from the work of Vanden-Broeck (1980) that  $d/F^2$  is bounded as  $F^2 \rightarrow 0$ . Hence as  $F \rightarrow 0$ , solutions can only be found for increasingly small values of  $d$ . Further, in this limit the waves become quite steep, and are increasingly difficult to calculate with our present numerical method. Indeed, for the case  $d = 0.001$  shown in figure 6 we see a departure from the linearized theory when  $F < 0.1$ . As  $d$  is increased, the nonlinear effects emerge for larger  $F$ , see the discussion in the following paragraphs.

The case when  $d = 0.01$  is shown in figure 9. As the Froude number  $F$  nears unity, there are periodic wave solutions, including supercritical ones (in fact, these solutions also exist for the case  $d = 0.001$ ). The wave solutions when  $F > 1$  have very long wavelengths and large amplitudes. When  $F \approx 1$  the linearized theory using either method 1 or 2

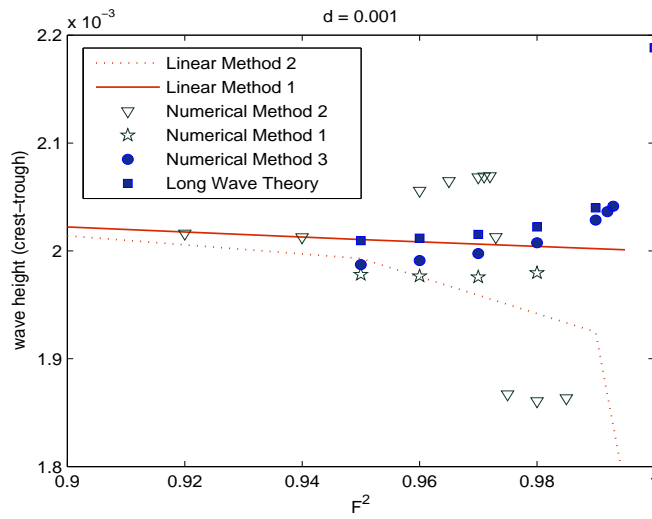


FIGURE 8. Blow up of figure 6 when  $F^2$  nears 1.

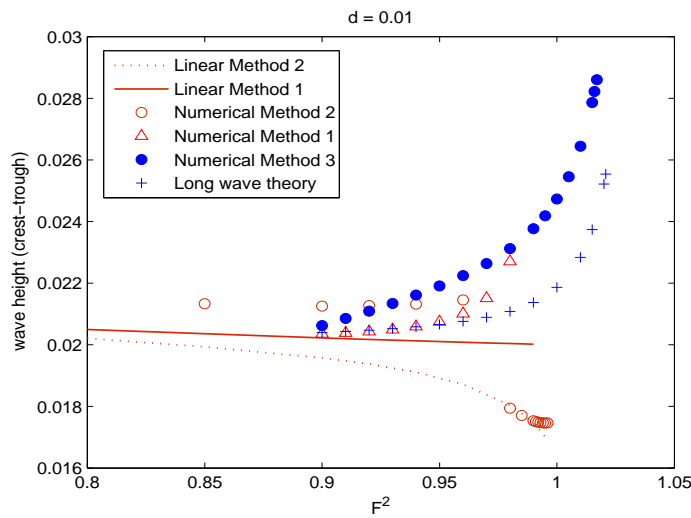
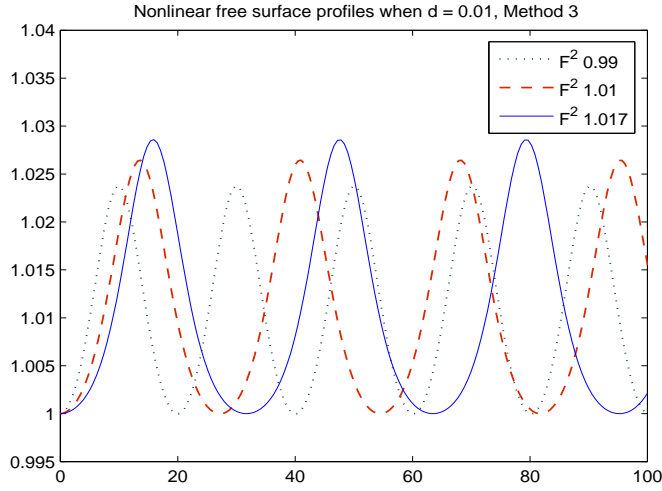
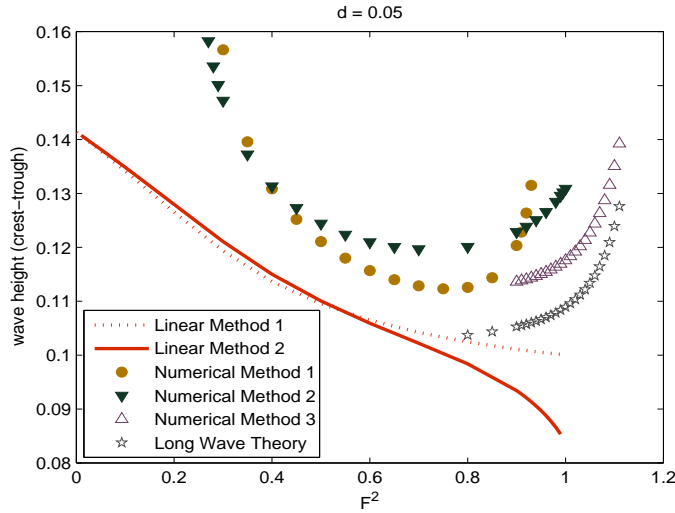


FIGURE 9. Relationship between wave height (crest-trough) and  $F^2$  when  $d = 0.01$ .

fail to predict the periodic waves. For these flows, we obtain better numerical results by using the wavelength from the long wave analysis (method 3). As  $F$  increases, the wave amplitude and wavelength increase, and the amplitude increases rapidly when  $F$  is only slightly greater than unity. More mesh points are then needed in the numerical calculations. Some typical free surface profiles by method 3 are shown in figure 10.

The case when  $d = 0.05$  is shown in figure 11. Now the difference between the linearized theory and the numerical results can be clearly seen. As the  $F$  decreases to zero, the amplitude of nonlinear waves increases rapidly, especially when  $F^2 \rightarrow 0.3$ . We were unable to obtain convergence of the numerical solution when  $F^2 < 0.2$ . When we increase  $F^2$  towards unity, the wave amplitudes also increase. Similarly for the cases of smaller  $d$ , the linearized theory fail to predict periodic waves for  $F^2 \rightarrow 1$ . Thus method 3 is used to get the corrected wavelength when  $F \approx 1$ . The numerically determined waves can be

FIGURE 10. Free surface profiles when  $d = 0.01$ .FIGURE 11. Relationship between wave height (crest-trough) and  $F^2$  when  $d = 0.05$ .

extended continuously at  $F^2 = 0.9$  from the solutions obtained by method 1 (linearized theory) which gives a good approximation for the range of  $0.3 \leq F^2 \leq 0.8$ .

Finally, the case of  $d = 0.1$  is shown in figure 12. For this relatively large  $d$ , the results from the linearized theory and the long wave analysis do not agree with our numerical results, but they still have the same trend. We found that the numerical solutions converge only for a finite range of Froude number, smaller than for the case of  $d = 0.05$ .

Next we investigate the case when  $d < 0$  noting that the weakly nonlinear long-wave analysis of section 3.3 suggests that waves can then be found for  $F < 1 + d$ , which is always subcritical. Fixing  $d < 0$ , the wavelength of these waves increases whereas the amplitude decreases as  $F$  increases. For  $d = -0.01$ , some typical nonlinear free surface profiles are shown in figure 13 whereas the relationship between wave height and  $F^2$  is shown in figure 14. The results from the long-wave analysis are in good agreement with

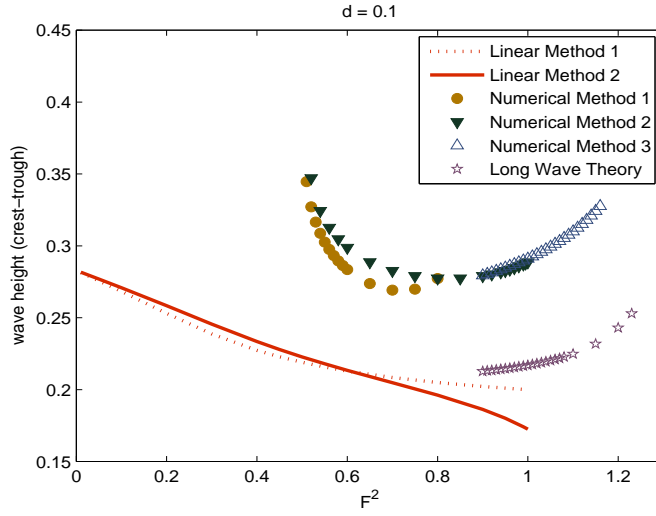


FIGURE 12. Relationship between wave height (crest-trough) and  $F^2$  when  $d = 0.1$ .

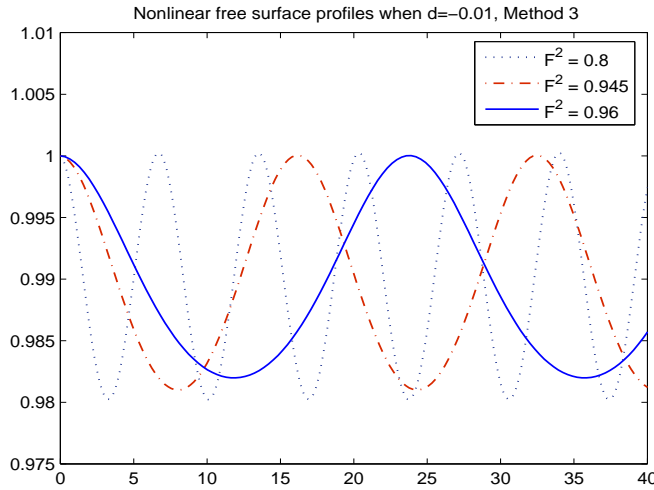
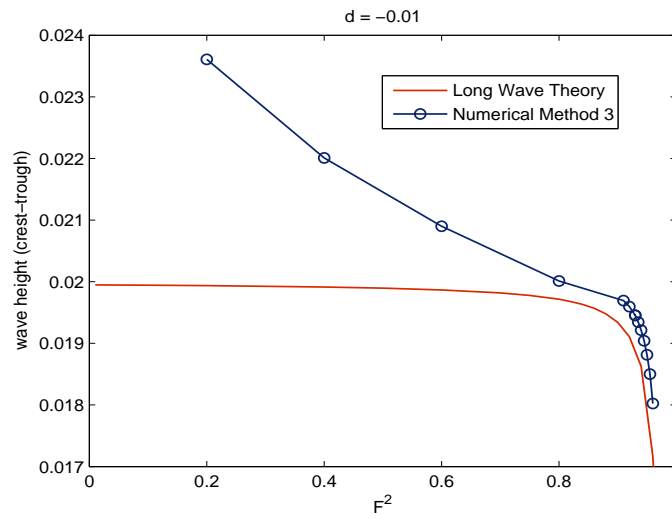
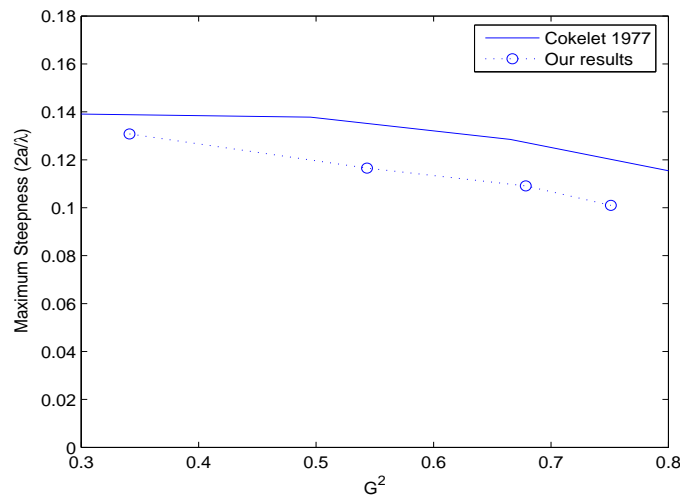


FIGURE 13. Nonlinear free surface profiles when  $d = -0.01$  for various values of  $F^2$ .

the numerical results as  $F$  approaches  $1 + d$ . As expected, the discrepancy increases as  $F$  decreases. From the long-wave analysis of section 3.3, this periodic wave approaches a limiting solution which is one-half of a solitary wave as  $F \rightarrow 1 + d$ . This solution is discussed later in section 5.3.

### 5.2. Highest wave

Using our numerical method, for each fixed  $F$  considered, we increased  $d > 0$  until the iteration failed to converge. This yielded the wave of maximum steepness we were able to obtain. The relationship between the maximum steepness  $2a/\lambda$  and the *downstream* Froude number  $G^2$  is shown in figure 15, where we also plot the corresponding results from Cokelet (1977), as discussed in section 3.5. A typical free surface profile when  $G^2 = 0.5434$  is shown in figure 16. The difference between Cokelet's results and our

FIGURE 14. Relationship between wave height (crest-trough) and  $F^2$  when  $d = -0.01$ .FIGURE 15. Relationship between maximum steepness and  $G^2$ 

results is due to our difficulty in computing very steep waves. The accuracy of numerical solutions is improved by increasing the number of mesh points per one wavelength. But note that, as  $G^2$  increases, the accuracy loss in our computation is compounded since we have to calculate many wavelengths, whereas Cokelet (1977) computed only one wavelength. The solution shown in figure 16 is obtained by using 60 mesh points per one wavelength and we integrate over 11 wavelengths. Note that these nonlinear waves have broad troughs and narrow crests, as the highest obtainable wave is reached.

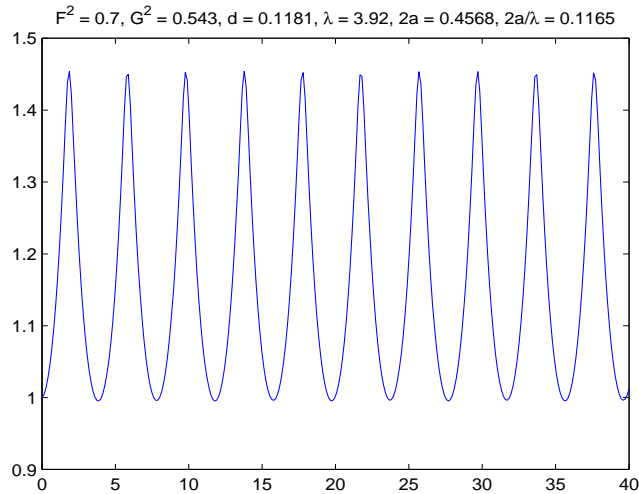
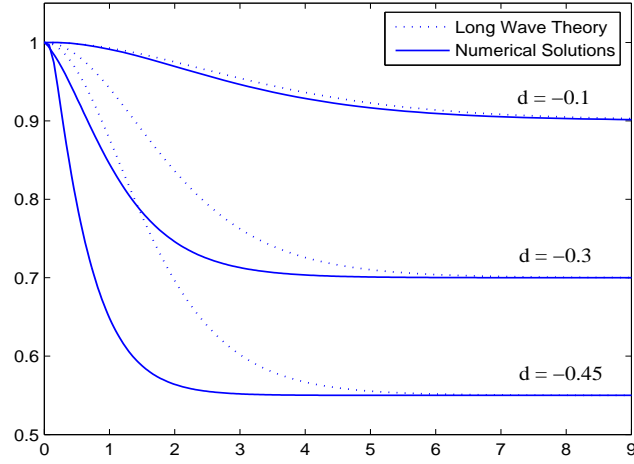
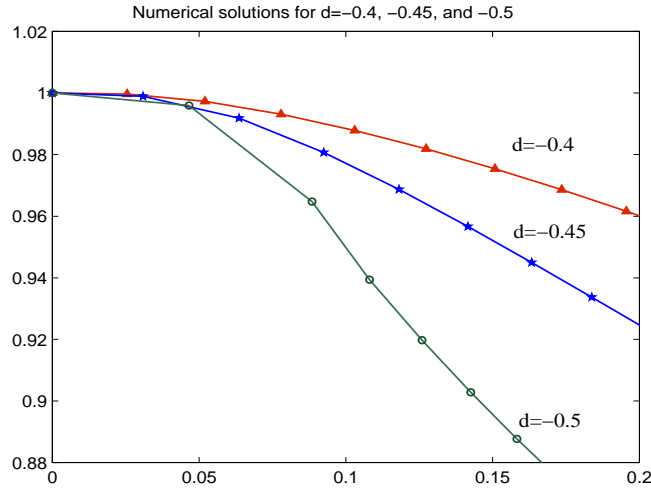


FIGURE 16. Free surface profile for  $G^2 = 0.5434$ ,  $F^2 = 0.7$ ,  $d = 0.1181$ .

### 5.3. Wave-free solution

In section 3.1 we showed that a wave free solution exists only when  $F^2 = (1 + d)^2$ , or  $G^2 = 1/1 + d$ . Since we expect to find wave-free solutions only for downstream supercritical flows, this implies that such solutions can only exist for  $d < 0$ . This result was confirmed by the weakly-nonlinear long-wave analysis of section 3.3, where it was shown that such wave-free solutions are just one-half of a solitary wave, except in a small region near the plate edge, where the local analysis of section 3.4 shows that there is a weak singularity. Our numerical results for various values of  $d < 0$  are shown in figure 17, and shows very good agreement with the long-wave theory when  $|d|$  is small. In the numerical calculations, we can find such wave-free solutions for a range of  $F_c < F < 1$  and corresponding  $d_c < d < 0$ . However, numerically we were unable to find any such wave-free solutions when  $d > 0$ . This is to be expected since these wave-free solutions are in fact well approximated by one-half of a solitary wave, which being always an elevation wave, can only accommodate the boundary condition at the plate edge when  $d < 0$ . Note that for these wave-free solutions, the ratio of the amplitude to the depth is  $|d|/1 + d$ . But for the solitary wave of maximum height this ratio is 0.833, which suggests that the interpretation of these wave-free solutions as one-half of a solitary wave is only valid for at most  $-0.454 < d < 0$ . Thus, on theoretical grounds we estimate that the cut-off value  $d_c = -0.454$ . This is confirmed by our numerical results, where as  $-d$  increases above 0.454 we find increasing difficulty in satisfying the condition at the plate edge that  $h_x = 0$  at  $x = 0, y = 1$ . In figure 18 we show a close-up of the wave-free profiles for a set of values of  $d$  around  $-0.454$ , which shows that the slope near the plate edge increases sharply when  $d < -0.45$ . For values of  $d < -0.5$  the wave-profile develops a completely unacceptable sharp slope at the plate edge. We also note here that these wave-free solutions are constrained by the requirement that the downstream Froude number  $G$  satisfies  $G^2 = 1/1 + d$ , which is only asymptotically correct for a solitary wave as  $d \rightarrow 0$  (in fact it is correct to the first order in  $d$ ). For the highest solitary wave  $G^2 = 1.666$  and this yields an alternative estimate of  $d_c = -0.4$ .

FIGURE 17. Wave-free profiles for various values of  $d < 0$ .FIGURE 18. A close-up of wave-free profiles for various values of  $d$  around  $-0.454$ .

## 6. Summary and discussion

We have presented numerical results for the calculation of the periodic waves generated by a steady free surface flow under a semi-infinite flat plate in water of finite depth. Gravity is included but surface tension is neglected in the dynamic free-surface boundary condition. When the draft  $d$  of the depressed plate is small, we have compared our numerical results with the linearized theory, where we used conservation of momentum to calculate the downstream wave amplitude, with very good agreement, provided that the upstream Froude number  $F$ ,  $0 < F < 1$  is not too close to either zero or unity. When  $F \rightarrow 0$ , the problem needs to be rescaled to what is essentially a deep-water formulation. As  $F \rightarrow 1$ , the periodic waves have long wavelengths, and so have used a weakly-nonlinear long-wave asymptotic theory to obtain some analytical results.

Nonlinear waves have been found numerically. Our numerical method specifies the draft  $d$  by the requirement that the downstream mean depth is specified, and this procedure requires us to input the wavelength. We used three methods: linear method in which the wavelength is determined from the linear dispersion relation for ( $d = 0$ ), a linear method based on the dispersion relation for ( $d \neq 0$ ), and the weakly-nonlinear long-wave determination of the wavelength. This flexibility enabled us to obtain nonlinear results for both subcritical and supercritical flows, particular in the regime when  $F \approx 1$ . As  $d$  gets larger, the downstream periodic waves become steeper, and eventually reach limiting waves with narrow crests and broad troughs. We have favourably compared the highest waves we can obtain with previous results for the periodic wave of maximum height. We have found downstream periodic waves for both  $d > 0$  and  $d < 0$ . For  $d > 0$ , the wave amplitude for each fixed  $d$  increases as  $F \rightarrow 1$  and as  $F \rightarrow 0$ . But for  $d < 0$ , the wave amplitude decreases as  $F$  increases towards the limiting value of  $F = 1 + d$ . At this value, downstream wave-free solutions are predicted to occur, and indeed we found such solutions for the range  $F_c < F < 1$  where the cut-off  $F_c$  is estimated to be around the value  $F_c = 0.546$  corresponding to the estimated value of  $d_c = -0.454$ , obtained from the known highest solitary wave height. They have the appearance of one-half of a solitary wave, in agreement with the weakly nonlinear long-wave analysis, valid as  $F \approx 1$ .

The problem we have considered here is rather simplified. We have included only the effects of gravity on the free surface, and a more complete treatment would involve also including surface tension. Also, the plate is semi-infinite in extent, and it may be interesting to consider flow under a plate of finite length.

The second author would like to thank Assoc. Prof. Jack Asavanant at the Chulalongkorn University for some useful comments on the numerical method. This research was financially supported by the Thailand Research Fund to the second author.

## REFERENCES

- ANDERSSON, C. D. & VANDEN-BROECK, J.M. 1996 Bow flows with surface tension. *Proc. R. Soc. Lond. A* **452**, 1985–1997.
- COKELET, E. D. 1977 Steep gravity waves in water of arbitrary uniform depth. *Phil. Trans. R. Soc. Lond. A* **286**, 183–230.
- HOCKING, G. C. 1993 Bow flows with smooth separation in water of finite depth. *J. Austral. Math. Soc. B* **35**, 114–126.
- MALEEWONG, M., GRIMSHAW, R. & ASAVANANT, J. 2005 Free surface flow under gravity and surface tension due to an applied pressure distribution in bond number greater than one-third. *Theor. Comput. Fluid Dyn.* **19**, 237–252.
- MCCUE, S. W. & STUMP, D. M. 2000 Linear stern waves in finite depth channels. *Q. Jl Mech. appl. Math.* **53**, 629–643.
- SCHMIDT, G. H. 1981 Linearised stern flow of a two-dimensional shallow-draft ship. *J. Ship Res.* **25**, 236–242.
- TOOLEY, S. & VANDEN-BROECK, J. M. 2004 Capillary waves past a flat plate in water of finite depth. *IMA J. Appl. Math.* **69**, 259–269.
- VANDEN-BROECK, J. M. 1980 Nonlinear stern waves. *J. Fluid Mech.* **96**, 603–611.
- VANDEN-BROECK, J. M. & KELLER, J. B. 1987 Weir flows. *J. Fluid Mech.* **176**, 283–293.